Robust methodology to simulate real shot peening process using discrete-continuum coupling method

Mohamed JEBAHI[a,b,*], Augustin GAKWAYA[a], Julie LÉVESQUE[a], Oussama MECHRI[a], Kadiata BA[a]

[a] *Laval University, 1065 Avenue de la Médecine, G1V 0A6, Québec, Canada*
[b] *Arts et Metiers ParisTech, I2M, UMR 5295 CNRS F-33400, Talence, France*

Abstract

Shot peening is widely used in automotive and aeronautic industries to improve fatigue life of metallic components. Its beneficial effects are mainly due to the residual stress field caused by the plastic deformation of the near-surface region resulting from multiple shot impacts. It is therefore important to know the values of the induced residual stresses in order to predict the mechanical strength of the peened component, and to know how these stresses vary by changing the shot peening parameters. The problem is that experimental measurement of residual stress is costly and time-consuming, and generally involves semi-destructive techniques. These difficulties make assessment of compressive residual stresses in real (industrial) peened components very challenging. On the contrary, numerical simulation can provide an alternative way to deal with this task. Consequently, several shot peening models have been developed in the literature. Although these models were successfully applied to investigate important physical phenomena encountered in shot peening, their application to assess residual stresses resulting from a real shot peening test is still not within reach. Indeed, due to computation costs and the complexity of the process, they cannot be directly applied to simulate a complete shot peening experiment. Development of a robust methodology allowing these models to properly simulate such an experiment at minimal cost (*i.e.* using simplifying assumptions) is thus needed. The present paper aims to meet this need. First, a new discrete-continuum coupling model combining the strengths of the existing shot peening models was developed. To avoid expensive computation times, only major shot peening features are included in this model. Then, a comprehensive methodology explaining how this model can be applied to simulate a real shot peening experiment was proposed. To validate the developed model as well as the associated methodology, they were applied to simulate a real shot peening experiment from the literature. Relatively good results were obtained compared to experimental ones, with relatively little computation effort.

Keywords: Shot peening, residual stress, Almen intensity, saturation, methodology, discrete-continuum coupling

1. Introduction

To improve life expectancy, durability and operating performance of metallic components, different methods can be applied. Generally, these methods include use of expensive advanced materials having higher mechanical strength, modifying the operating conditions (environment, loading, *etc.*) or simply enhancing the near-surface properties by introducing compressive residual stresses (CRS) in this region. In addition to its effectiveness, the last method seems to be the least expensive, which explains the great scientific interest in it. Consequently, several surface treatment techniques have been developed in this context. An overview of these techniques can be found in reference [1]. One of them is shot peening (SP) which is widely used to improve fatigue life of metallic components in automotive and aerospace industries due to its economical cost and applicability to various targets. This process entails bombarding a surface of metallic component with small spherical shots at high velocities ($20 - 100\,\mathrm{m/s}$). Each shot acts as a tiny ball-peen hammer that compresses and stretches the component surface. After each impingement, an indentation surrounded by a plastic region is created. The near-surface plastic strain generated during

*Corresponding author
Email address: mohamed.JEBAHI@ensam.eu (Mohamed JEBAHI)

shot peening leads to a residual stress profile through the thickness. The residual stress is compressive at the top surface and tensile underneath the surface of the component to ensure the mechanical equilibrium. The surface work hardening and the compressive residual stress induced by shot peening allow to hinder crack propagation, as cracks originate mostly from the surface. This can improve fatigue life and resistance to stress corrosion cracking within the peened component [2, 3, 4]. However, the beneficial effects of this process are conditional upon respecting several conditions. Indeed, numerous shot peening parameters can hugely influence the effectiveness of this process [5, 6]. For example, over- or under-peening can result in adverse effects on fatigue strength. Selection of the most suitable and optimal parameters to achieve an expected degree of improvement is always a matter of question in the designer mind. Such a question has received a great deal of interest over the years and significant amount of research has been done in understanding such a process.

Several researchers have used the experimental way to study shot peening. Lieurade and Bignonnet [7] and Wohlfahrt [8] have studied the fundamental mechanisms of shot peening. Mainly two mechanisms are at the origin of CRS: Hertzian pressure due to normal impact forces and surface stretching (enlargement) due to tangential impact forces. The fatigue performance not only depends on the CRS at the top surface, but also on the gradient inside the material. Maeder *et al.* [9] have investigated the influence of the most important SP parameters on the peening-induced residual stress. Three categories of SP parameters can be distinguished: process parameters, *e.g.* Almen intensity and exposure time, component parameters, *e.g.* component material, and shot parameters, *e.g.* size , material, velocity and impact angle of shots. Kobayashi *et al.* [10] have studied the difference between static and dynamic indentation tests using single and multiple shots. Static indentation is quite different from dynamic one, probably due to high strain rate effects. In dynamic indentation, single shot leads to tensile stress at the indentation center, whereas compressive stress is found in static indentation. The compressive stress induced by shot peening (dynamic impacts) is due to superimposition of residual stresses generated by impacts performed around each other. For more details of the experimental works, the reader is referred to reference [11]. Despite its effectiveness, the experimental way suffers from several difficulties related to the cost of experiments.

To avoid experimental difficulties, other researchers have proposed to study analytically the CRS in the peening component. Al-Hassani [12, 13] and Guagliano [14] have proposed an analytical relationship between the peening-induced arc height and the residual stress profile in thin components, using tensile force and bending moment internally generated to equilibrate the total peening-induced stress. Guechichi [15] has proposed simplified formulas to predict the maximal value and the depth of the CRS field, using Hertz contact and elastic-plastic theories [16]. These formulas were later improved by considering different constitutive laws for the target material [17] and by considering the effect of the tangential friction between the shot and the target [18]. Li *et al.* [19] have proposed a simplified analytical model to calculate the CRS field due to shot peening in semi-infinite target components. This model was improved by Shen *et al.* [20] to take into account more shot peening parameters, such as size and velocity of the shots and material of the target component. Recently, Miao *et al.* [21] have proposed a combined analytical model, including models of Li *et al.* [19], Shen *et al.* [20] and Guagliano [14], to investigate the influence of the shot peening parameters on the resulting Almen intensity and on the residual stress in an Almen strip. Several other analytical models can be found in the literature, of which an overview is provided in reference [11]. Compared to experiments, the analytical models are much less expensive. However, they are generally based on simplifying assumptions which can affect their effectiveness. Furthermore, obtaining analytical solution from these models is often very mathematically challenging, especially when complex structures are involved.

With the help of the increasing computer power, numerical simulation have become an effective method to investigate the shot peening process. Consequently, several numerical models have been proposed in the literature [14, 22, 23, 24, 25]. An extended review of these models will be given in section 2. The first numerical models developed in the literature consider only one shot impacting a target surface. Although they are extremely simplistic, these models allowed a better understanding of several physical phenomena encountered in shot peening. To study the influence of multiple impacts on SP results, other researchers have proposed models with multiple shots having initial ordered configuration. More recently, these models have been improved by considering randomly generated shots. Further improvements have proposed more complex SP models to take into account more complex mechanisms, such as interaction between shots, fluctuation of shot velocities and impact angles, shots deformation, thermal behavior of shots and target component, *etc.* [24, 26, 27]. The problem with application of

complex SP models is that the computation time is an increasing function of the complexity of the involved SP phenomena. For instance, taking into account shot-shot interactions results in a computation time proportional to N^N, where N is the number of shots, which is much larger than that obtained when ignoring such interactions (the associated computation time is simply proportional to N). Therefore, although complex SP models generally guarantee a more efficient representativeness of a real SP process, their application to predict residual stresses resulting from a real SP experiment remains very challenging. Simulation of a complete SP test using such models can lead to unaffordable computation times. The challenge here is how to properly simulate a real SP experiment whilst keeping acceptable computation time. In other words, is it possible to correctly assess important results from a real SP test using a simplified numerical model that includes only major SP phenomena? The present paper aims to tackle this challenge. Based on the different (experimental, analytical and numerical) works on shot peening, this paper proposes an effective approach to properly predict the peening-induced residual stresses in a real shot peeing test with minimal computation effort. This approach consists of two parts:

- development of a simplified shot peening model based on simplifying assumptions to avoid large computation costs (only major SP mechanisms must be taken into account in this model). It should be noted that this model is similar to those proposed in the literature. And then,
- development of a robust and comprehensive methodology explaining how this simplified model can predict peening-induced residual stresses in a real (industrial) shot peening experiment.

As shown in the literature [25, 28], for given shot type and impingement angle, the Almen intensity and exposure time are major indicators that ensure the effectiveness and repeatability of a given SP experiment. In other words, for given shot type and impingement angle, the SP results depend almost solely on these parameters (Almen intensity and the exposure time), and not on how individual shots impact the target component [25, 28]. Using this finding, the key idea of the proposed methodology is then to satisfy the same repeatability conditions (Almen intensity and the exposure time) between the considered experiment and the associated simplified model. As will be explained later, it is not necessary to take into account all the complex and time-consuming SP mechanisms to correctly model a real SP experiment. The effects of such mechanisms can be considered indirectly by application of the proposed methodology which represents the major novelty of the present paper.

Following this introduction, this paper is divided into five sections. Section 2 gives an overview of the different classes of the SP numerical models developed in the literature. Based on this review, a new model combining the strengths of these classes, while alleviating their drawbacks, is proposed. A 3D random discrete-continuum coupling model between the discrete element method (DEM) [29, 30] and the finite element method (FEM) [31] is developed in this section. This model considers only major SP mechanisms. Section 3 provides a comprehensive methodology allowing the proposed model to properly simulate a real shot peening process. This methodology is based on the determination of control curves relating the shot velocity to the Almen intensity. Section 4 shows how these curves can be determined for given Almen strip, shot type and impingement angle. Section 5 aims to validate the developed methodology by simulating a real shot peening test from the literature. As will be seen, relatively good results are obtained. Section 6 presents some conclusions.

2. 3D random discrete-continuum coupling model

Numerical simulation have become increasingly used since the 1970s to investigate, understand, explain and predict the correlation between the influencing SP parameters and the process results. Consequently, several numerical models have been published in the literature. In order to develop a numerical tool including the strengths of such models, a birdeye view of the models most commonly used is given hereafter.

2.1. Brief review of shot peening numerical models

First classification of the existing numerical models enables differentiation between $2D$ and $3D$ models. Due to their simplicity, $2D$ axis-symmetric models are very popular to investigate single-shot impact on cylindrical and semi infinite target components [32, 33, 34]. Although they are very simplistic, these models have allowed

to investigate qualitatively several important physical phenomena encountered in shot peening, such as influence of the shot deformation behavior on the SP results [35, 36]. However, quantitative comparison of the associated numerical results with experimental ones proves that they misestimate the experimental results. Furthermore, effects of inclined and multiple-shot impacts cannot be taken into account with such models.

To circumvent these limitations, $3D$ models have been proposed in the literature. These models can be divided into single-shot and multiple-shot models. The single-shot models have been developed to investigate in a simple way the $3D$ effects of normal and inclined single impact on the residual stress profile. Application of such models has yielded an important conclusion concerning the shot mechanical behavior. Guagliano [14] has shown by simulation of single impact on an Almen strip that results obtained using a rigid shot are close to those obtained using a deformable elastic one. This conclusion can be generalized to other target materials having low yield and hardness values, *e.g.* aluminum alloys [37], compared to those of the shot material. Despite their simplicity and economical cost, the single-shot models are overly simplified and cannot be used to simulate real SP test. As stated by Kobayashia *et al.* [10], single-shot impact leads to near-surface tensile residual stress, which contradicts the SP aim. The compressive residual stress obtained during shot peening is due to effects of multiple impacts [10]. To take into account these effects, researchers have proposed multiple-shot models. The first models in this category consider prior positioning (ordered) shots [38, 39]. Using ordered configuration of shots, it is straightforward to model the target component which can easily be represented by a periodic unit cell with symmetric boundary conditions. Different techniques have been proposed in the literature to choose the unit cell of the target component [23, 24, 14]. The ordered-shot models have been widely applied to study different SP mechanical aspects. Two important results can be recalled here. The first result concerns the Coulomb friction coefficient μ used to describe the tangential interaction between shots and the target component. Meguid *et al.* [28] have demonstrated that for $0.1 < \mu < 0.5$ the friction effect on both plastic strain and compressive stress is very minimal. Similar result has been also obtained by Gariépy *et al.* [37]. The second result concerns the mechanical behavior of the target component. Bhuvaraghan *et al.* [22] have shown that shot peening can involve very high strain rates ($\dot{\varepsilon} = 10^5\ s^{-1}$) and then strain rate dependent properties must be taken into account in the target component model. Concerning thermal properties, contrary statements have been reported in the literature whether thermal effects have to be considered in a realistic SP model. Several authors [40, 41] state that no thermal conduction takes place and all induced heat energy is retained in the deformed region, while others hold the opposite view [42]. A systematical study of such effects is still missing. Models with prior positioning shots have enabled researchers to take a great step towards quantitative modeling of a real SP process, since most of the SP phenomena are taken into account in them. However, these models do not consider the random aspect of the shots, which makes them not very representative of a real SP test. To overcome this limitation, several researchers have proposed random SP models in which shots are randomly generated.

Most of the proposed random SP models in the literature are based on the finite element method which is used to describe the mechanical behavior of both the shots and the target component [25, 43, 44]. From shots positioning point of view, these models provides a realistic representation of a shot peening process. However, they are time-consuming and can only be applied when a small number of shots is used, which can affect their ability to correctly model a shot peening experiment. Recently, some researchers have explored the discrete element method (DEM) coupled with the finite element method (FEM) as an alternative approach to increase the number of shots in the SP simulation [45]. In this approach, the shots assumed to be rigid are modeled with DEM, whereas the target component is modeled by FEM to properly describe its mechanical behavior. Since the shot yield and harness must be larger than those of the target component to ensure beneficial SP effects, the rigid body assumption of the shots can be justified [25, 46]. Using the DEM-FEM approach, it would be possible to model large number of shots which are only represented by their density, radius and gravity centers (no mesh is needed). Based on this approach, several SP models have been developed in the literature to take into account more complex SP phenomena, and then to more closely mimic a real shot peening process. In this respect, researchers have proposed advanced interaction laws to take into account the effect of shot-shot interactions [24, 26, 27]. In an interesting work, Murugaratnam et al. [27] have also considered in their model the effect of material hardening, by dynamically adapting the coefficient of restitution for repeated impacts on the same spot. Other SP models taking into account more complex SP phenomena can be found in the literature. The major drawback of these models is that they can entail large

calculation effort, which can limit their application to small target components. Indeed, some SP phenomena such as shot-shot interactions are time-consuming and can dramatically increase the computation time, especially when a large number of shots is used. Therefore, a trade-off must be found between the SP phenomena to be considered and the resulting computation effort.

The random DEM-FEM coupling approach will be employed in the following. Because, almost all the major SP mechanical phenomena are taken into account in this model. Furthermore, a large number of shots can be modeled without increasing dramatically the computation time, especially when shot-shot interactions are ignored. Depending on the exposure time of the SP test to be modeled, it may be necessary to simulate a large number of shots with this model. Therefore, to avoid unaffordable computation times, only shot-component interactions are considered in this model. In this case, the simulated shot stream can be interpreted as an effective stream. As will be seen later, modeling only the effective shot stream can be sufficient to correctly predict important experimental results.

2.2. Proposed 3D random DEM-FEM coupling model

During a shot peening experiment, large numbers of shots impact the treated component at random positions and in a random sequence. This paper proposes a 3D random DEM-FEM coupling approach to more closely mimic a real shot peening process (fig. 1). This model is constructed using the recent version of the commercial code *Abaqus* Explicit 6.13 which includes the discrete element method (DEM).

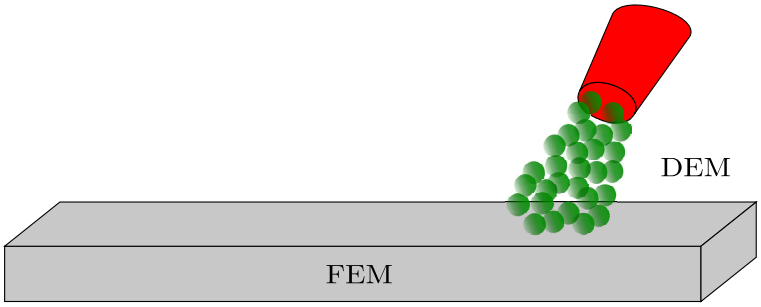

Figure 1: 3D random DEM-FEM coupling approach to simulate real shot peening

The target component is modeled via FEM. Since very high strain rates are involved in shot peening, rate-dependent properties must be taken into account in the target component model. Several approaches have been proposed in the literature to handle strain rates. Among them, the isotropic hardening approach with rate-dependent properties is widely used to model the mechanical response of numerous materials concerned by shot peening, *e.g.* aluminum alloys and spring steels (Almen strip material). Based on the work of Bhuvaraghana *et al.* [22], this approach correctly predict the mechanical response of an Almen strip. Therefore, it is retained in this paper. From the mathematical techniques used to model isotropic hardening with rate-dependent properties, the Johnson-Cook equation is employed to describe the Von Mises stress σ flow as function of the equivalent plastic strain ε:

$$\sigma = \left[A + B\,\varepsilon^{n}\right]\left[1 - C\ln\left(\dot{\varepsilon}^{*}\right)\right]\left[1 - T^{*\,m}\right] \tag{1}$$

where A, B, C, n and m are the five Johnson-Cook constants to be determined experimentally, $\dot{\varepsilon}^{*}$ is the dimensionless strain rate defined as $\dot{\varepsilon}/\dot{\varepsilon}_0$, $\dot{\varepsilon}$ and $\dot{\varepsilon}_0$ are respectively the current and reference strain rate, T^{*} is the homologous temperature defined as $(T - T_{room})\,/\,(T_{melt} - T_{room})$, T_{room} and T_{melt} are respectively the room and melting temperature. In addition to the strain rate effects, this equation can also take into account the thermal effects by using a nonzero m.

For the reasons stated in the previous subsection, the shots are assumed to be identical rigid spheres. In a DEM simulation, these elements are only represented by their density ρ_s, radius R and the coordinates of their centers (x, y, z). In order to randomly generate the coordinates of each shot center, a *Python* program is developed and connected to *Abaqus*. This program requires as inputs the peening surface, shot number N and radius R. For practical purposes, the origin of the coordinate system is chosen as the center of the peening surface. The z-axis

is normal to this surface and directed towards the target component. Assuming a $2\,a \times 2\,b$ surface, in the case of normal impacts, the coordinates of each shot center are obtained by:

$$\begin{cases} x &= & a\ (2\,\text{random}\,() - 1) \\ y &= & b\ (2\,\text{random}\,() - 1) \\ z &= - & R\ (1 + 2\ (N - 1)\ \text{random}\,()) \end{cases} \tag{2}$$

where random () is a uniform pseudo-random number generator in the interval [0, 1] (fig. 2a); in the case of oblique impacts, the centers are obtained by:

$$\begin{cases} z &= - & R\ (1 + 2\ (N - 1)\ \text{random}\,()) \\ y &= & b\ (2\,\text{random}\,() - 1) \\ x &= & a\ (2\,\text{random}\,() - 1) + (z - R)/\tan\,(\theta) \end{cases} \tag{3}$$

where θ is the impingement angle (fig. 2b). After generation of the center coordinates, spherical shots of radius R and density ρ_s are created and automatically sent by the *Python* program to the predefined *Abaqus* input file which already includes the target component model. Then, the desired velocity is applied to all the shots in the impingement direction, before introducing the component-shot interaction laws and the simulation starts. In fact, small fluctuations of shot velocities around an average value can occur in SP experiments. However, these fluctuations are generally unpredictable and very difficult to quantify with sufficient precision. For the sake of simplicity, these fluctuations are neglected in the present model, in which the same velocity value is applied to all the shots. It should be noted that this value can be different from the mean velocity of the flow measured experimentally. As will be seen in the proposed methodology, the shot velocity is numerically determined so as to ensure the expected Almen intensity (i.e. the Almen intensity of the modeled experiment), which is a major indicator of experiment repeatability. This is a way to offset the weakness of the proposed SP model due to the simplifying assumptions.

To model the shot-component interactions, the kinematic contact algorithm implemented in *Abaqus* is selected [47]. This algorithm is based on the technique of prediction/correction to prevent shot-component interpenetration. Concerning the frictional behavior, as reported in the literature, the friction coefficient μ has minimal influence on the SP results and a value $\mu = 0.2$ is generally used [25, 37, 28], the same value is used in this work. It should be recalled that collisions between shots are ignored in this paper. The simulated shot stream is regarded as an effective stream. Also, interpenetration between shots at the initial configuration is not allowed: the minimal distance between newly generated center and all the existing ones is $2\,R$, otherwise this center is deleted and replaced by another random center until satisfying the minimal distance condition.

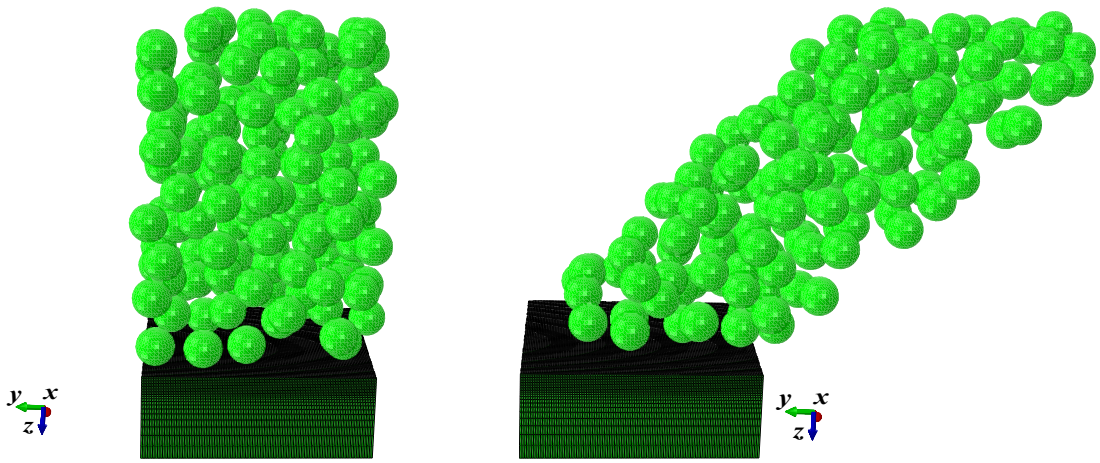

(a) Normal impacts $\theta = 90°$ (b) Oblique impacts $\theta = 45°$

Figure 2: Illustration of the 3D random DEM-FEM coupling model for normal and oblique impacts

Although most of the important physical phenomena encountered in shot peening are considered in the proposed DEM-FEM model, some time-consuming SP mechanisms (e.g. shot-shot interactions) are ignored to reduce the computation effort. But even so, application of this model to directly simulate a real SP experiment can lead to large or even unaffordable computation time (e.g. in the case of a large geometry of the target component). Furthermore, due to the simplifying assumptions used in this model, the associated results can be poor and unsatisfactory compared to the experimental ones. A methodology allowing for overcoming these difficulties and making simulation of a real (industrial) shot peening experiment possible is then necessary. This is the subject of the following section.

3. Methodology to simulate real shot peening processes using the proposed SP model

In general, components requiring mechanical surface treatment by shot peening are relatively large. During a real shot peening test, these components are bombarded with a great number of shots (several million shots) for several minutes. Despite the accelerating progress in computer science and software technology, numerical simulation of an entire shot peening test is not yet possible. The previous section dealt with the development of a simplified DEM-FEM model ignoring some time-consuming SP mechanisms to reduce computational effort. This section attempts to present a methodology allowing for quantitative simulation of real shot peening tests using this model, while keeping acceptable computation time. This methodology includes two steps. The first step consists in reducing the geometry of the studied component by selecting sufficiently representative elementary volumes (REVs) of this component. The position and dimensions of these REVs will be discussed in subsection 3.1. The second step consists in finding the test-equivalent shot peening parameters to be applied on the REVs to represent the real SP test on the entire component. The test-equivalent shot peeing parameters must be determined so as to numerically satisfy the repeatability conditions of the modeled experiment. This step is the subject of subsection 3.2.

3.1. Representative elementary volumes (REVs)

Far from the stress raisers (boundary conditions, shaft shoulder, etc.), the peening-induced residual stresses must be uniform to avoid detrimental SP effects [11]. The uniformity of these stresses were verified numerically by Meguid *et al.* [28] using multiple-shot model. In practice, to ensure this property, the target component must be sufficiently exposed to the shot stream until an expected coverage level is reached. Generally, 100 % coverage is sufficient to develop uniform residual stresses. However, in many cases, the coverage needs to be more than 100 %, for example, to increase the thickness of the affected region and to increase the value and depth of the maximal compressive residual stress [9].

Taking into account the uniformity of residual stresses, simulation of shot peening on the entire component is reduced to simulation using representative elementary volumes (REVs). Number and position of these REVs must be chosen so as to correctly represent the initial component. Figure 3 presents the REVs for an I-shaped component. Four regions associated with different stress raisers can be distinguished. To completely represent this component, each of these regions must be represented by a REV. The residual stress profile in the entire component can be then obtained from REVs results using extrapolation techniques. As for the REVs dimensions, these quantities must be sufficiently small to reduce computation time, but sufficiently large for the average residual stress to be representative. In almost all the numerical models, the target component dimensions are arbitrary chosen, which can lead to sub-optimal SP results. Furthermore, the conventional method of convergence study (classically used in computational mechanics to determine the dimensions of a REV) requires prior knowledge of the simulation ingredients, which is not the case here. In effect, number and positions of the shots vary from a SP test to another one and they are very difficult to be predicted in advance. This paper proposes another numerical method to properly obtain the REVs dimensions.

To obtain the REV top surface (*i.e.* impact surface) dimensions, it is first proposed to determine the minimal distance between two shots d_{min} from which impacts do not influence each other, by simulating a series of two-shot impacts with different initial distances between shots. In this paper, impacts are considered as independent and

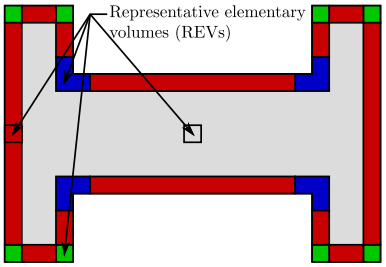

Figure 3: Representative elementary volumes (REVs) for an I-shaped component

having no influence on each other when the associated stress regions defined by (4) do not overlap:

$$\left\{ M \in \text{Top surface} \;\middle|\; \sigma^{ind}_{VM}(M) \geq 0.05\, \sigma^{ind}_{VM_{max}} \right\} \tag{4}$$

where $\sigma^{ind}_{VM}(M)$ is the Von Mises residual stress at a point M on the top surface and $\sigma^{ind}_{VM_{max}}$ is the maximal Von Mises residual stress in this surface. Then, the REV top surface is chosen as a square of $3\,d_{min}$ side (fig. 4). The choice of $3\,d_{min}$ here is justified by the fact that the measuring region ($d_{min} \times d_{min}$) located at the center of the REV top surface would not be disturbed by the boundary conditions. An impact outside the peening surface would not influence results at the measuring surface boundary. Concerning the REV thickness, this parameter is less sensitive to the number of shots and the classical convergence study method can be applied using a single-shot impact model to obtain such parameter.

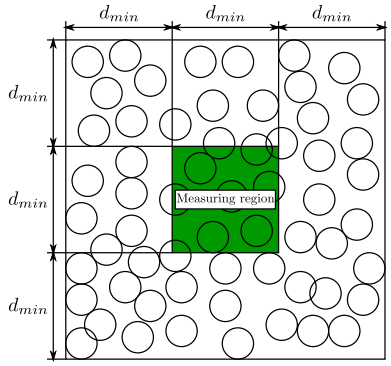

Figure 4: Top surface dimensions of the representative elementary volume (REV)

3.2. Test-equivalent shot peening parameters for the REVs

As seen in the introduction, several parameters are involved in shot peening and can greatly influence the associated results. The main parameters that must be taken into account to correctly model the SP process can be classified into three categories as follows:

- shot parameters: size, material, velocity and impact angle;
- component parameters: material, geometry;
- process parameters: Almen intensity and exposure time (or coverage).

The above shot parameters and component parameters are generally easy to model and do not change between using REV or the entire component (extrinsic to the numerical model). On the contrary, the process parameters (Almen intensity and exposure time) are more difficult to be taken into account in the SP model. In addition, the exposure time is highly dependent on the REV dimensions. Since these parameters ensure the effectiveness and repeatability of a given shot peening process [25, 28], they must be carefully taken into consideration in the SP numerical model. In the remainder of this subsection, it will be detailed how they can be modeled.

3.2.1. Almen intensity

This parameter is related to the amount of kinetic energy transferred from the shot stream to the target component during the shot peening process [5]. It was introduced by Almen [48] and can be determined by peening a number of Almen strips (clumped to a mounting fixture by means of four bolts) with the same SP parameters and different exposure times, according to SAE specifications [49, 50, 51]. An Almen strip is a standardized strip with given material (SAE 1070 spring steel) and dimensions (76 mm × 19 mm and three available thicknesses: $h = 0.79$ mm for type N , $h = 1.29$ mm for type A and $h = 2.39$ mm for type C). Once the bolts are removed, the peened strip will curve towards the peening direction. The resulting arc heights under different exposure times can be measured (fig. 5). The Almen intensity is defined as the arc height at saturation which is the point, on the curve of peening time versus arc height, beyond which the arc height increases by less than 10% when the exposure time doubles (fig. 6).

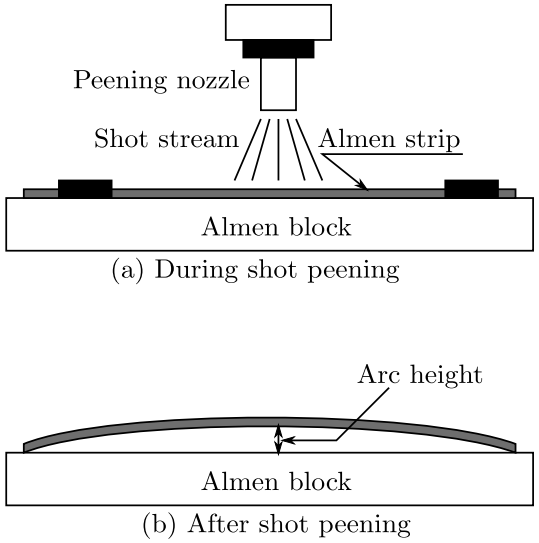

Figure 5: Shot peening of Almen strip for process control

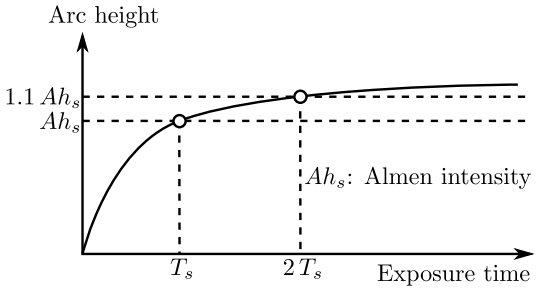

Figure 6: Shot peening saturation curve

As shown in several works [14, 22, 21], for a given Almen strip, this parameter mainly depends on the shot parameters (size, material, velocity and impact angle). Furthermore, for given shot type and impingement angle, this quantity depends nonlinearly on the shot velocity [22, 52]. To be able to take into account such parameter in the SP numerical model, it is therefore sufficient to find relationships relating this parameter to shot velocity for different types of shots and different impingement angles. Even if experimentally determined relationships between these two parameters can be found in the literature [22, 52], this paper proposes to search these relationships numerically using the simplified numerical model detailed in section 2. This can reduce errors due to numerical simplification of the real shot peening process. Indeed, using numerically obtained relationships (taking into account numerical simplifications) allows to determine the effective shot velocity (which can be slightly different from the experimental one) that leads to the experimentally measured Almen intensity. As Almen intensity is a key repeatability

indicator for a given shot peening process, the residual stress obtained with numerically determined shot velocity would be better than when using the experimental shot velocity.

The curves of Almen intensity as function of shot velocity for different types of shots and impact angles will be referred in this paper to as "control curves" (fig. 7). For the sake of clarity, the method to obtain these curves will be explained in a separate section (§4). It should be noted that obtaining these curves is very time-consuming since a great number of simulations must be performed. However, since standardized strips are used to measure the Almen intensity, such curves are independent of the target component and can therefore be used for any target component.

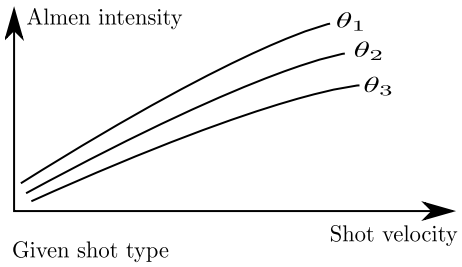

Figure 7: Shot peening control curves for given shot type and different impingement angles

3.2.2. Exposure time

In an interesting experimental work, Miao *et al.* [53] have demonstrated that the peening results obtained after one pass of a peening nozzle having relatively slow traveling velocity ($V = 10\,\mathrm{mm/s}$) are in close agreement with those obtained after 32 passes of the same nozzle when the traveling velocity is increased by a factor of 32 ($V = 320\,\mathrm{mm/s}$). It can be concluded from this statement that, for given shot parameters (size, material, velocity and impact angle), the peening results only depend on the number of shots impacting the considered component. Therefore, shot number can be used instead of exposure time to simulate a shot peening process. For a given SP test, exposure time is fixed in such a way as to ensure an expected coverage which is defined as the ratio of the area covered by peening indentations to the total area of treated surface, expressed in percentage. Thereby, it is sufficient to search the number of shots N_c that ensures the expected coverage value on the REV peening surface to take into account the exposure time in the numerical model. For a given REV, N_c can be determined numerically by simulating several shot peening tests using different numbers of shots (N). By determining the associated coverage values, relationships relating coverage to shot number can be obtained. These relationships can then be used to compute N_c for an expected coverage value. The question that arises here is how coverage can be assessed numerically.

Several numerical works studying the coverage effects on the SP results can be found in the literature [25, 44]. Most of them use plastic strain criteria to assess coverage. A point on the peening surface is considered to be within the impacted region when the associated plastic strain is larger then a given value. As shown by Miao *et al.* [25], such criteria can lead to poor results, especially in the case of oblique impacts. Since visual inspection is the standard method for coverage evaluation in SP experiments [54], this paper proposes a numerical method inspired by this technique. First, a single impact test using the same shot and component parameters as for the real SP process has to be simulated to determine the associated indentation area. This area can then be used to asses coverage for randomly scattered impact centers on the peening surface (fig. 8). A point on this surface is considered to be within the impacted region when it belongs to an indentation area associated with an impact center. In this work, an indentation area is chosen as explained in figure 8. In the case of general oblique impact, this area is delimited by an ellipse (circle in the case of normal impact) passing through the highest positions of the pile-up around the impact center. As will be seen, such a choice provides a good estimate of the coverage. Contrary to the existing coverage criteria, the proposed method naturally takes into account the non-symmetrical effects of oblique impact.

To simplify its application, the proposed method is automated using *Python* language. The developed *Python* program requires as inputs the number of shots N, the impingement angle, the individual indentation surface,

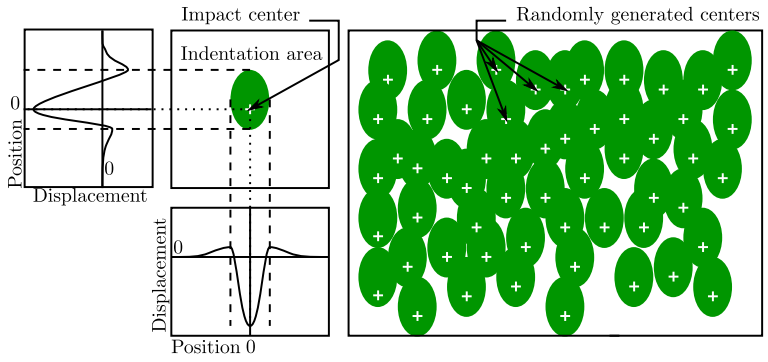

Figure 8: Numerical method to compute the shot peening coverage in the general case of oblique impact

the measuring surface and the total peening surface (on which the impact centers will be scattered). First, N shots locations are generated (eqs. (2) and (3)) and projected along the impingement direction onto the total peening surface which is discretized into a fine mesh with rectangular elements. Then, the measuring surface nodes located within indentation areas (associated with impact centers) are counted and recorded. Finally, the coverage is approximated by the ratio of the number of these nodes to the total number of nodes in the measuring surface. Applying this method, the coverage evolution with respect to the shot number is studied using a thin spring steel (Almen strip material) plate with 3.6 mm × 3.6 mm × 1.3 mm dimensions. In this study, two impingement angles $\theta = \{45°, 90°\}$ were used, the shot velocity is fixed at $V = 55\,\mathrm{m/s}$. Figures 9 and 10 show the corresponding indentation areas obtained after one impact.

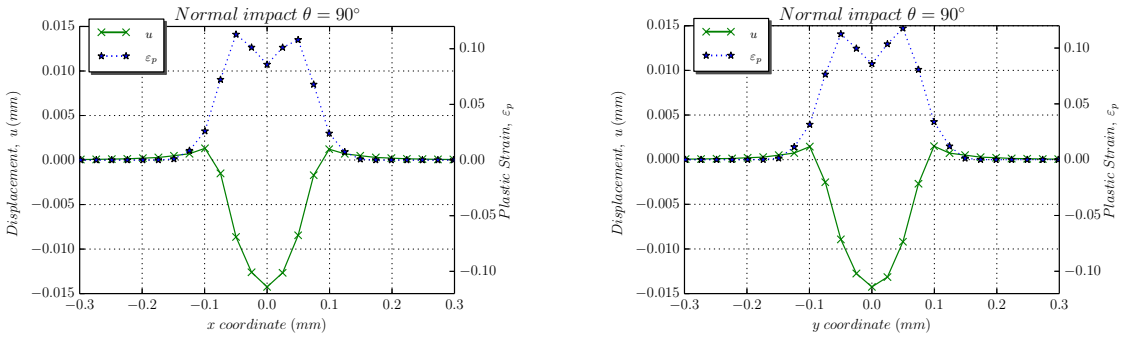

Figure 9: Indentation area after one normal impact at $V = 55\,\mathrm{m/s}$ velocity

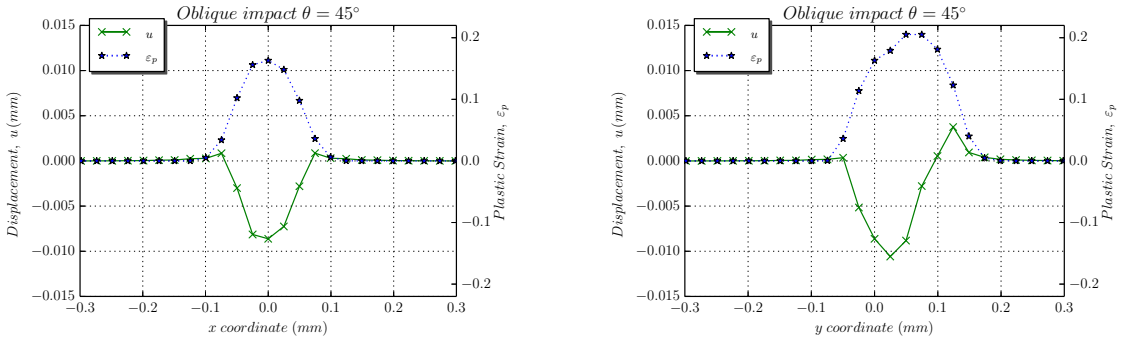

Figure 10: Indentation area after one oblique impact with $\theta = 45°$ at $V = 55\,\mathrm{m/s}$ velocity

Using these individual areas, the coverage evolution in the measuring zone (1.2 mm × 1.2 mm square at center of the peening surface) with respect to shot number N can be obtained (fig. 11). To study the random aspects, 6

different sequences of shots were generated for each N. As shown in figure 11, the results dispersion due to random generation of shots has tendency to decrease as N increases. Therefore, when a sufficient number of shots is used (to ensure 100% coverage or more), the random effects would be negligible. This will be confirmed in section 5. In a similar way as when using exposure time [55, 56], the coverage evolution as function of N can be expressed using an Avrami equation as:

$$C(N) = 100\left(1 - e^{-A\,N}\right) \tag{5}$$

with A is a nonnegative real constant which can be determined by the Moving Least Square (MLS) method. Using (5), the number of shots that ensures an expected coverage value N_c can be determined. As in experimental SP process, the number of shots corresponding to 98 % coverage is considered as a full coverage number N_f. Beyond 100 % coverage, the associated N_c is determined based on N_f. For example, 200 % coverage corresponds to $N_c = 2\,N_f$ shots.

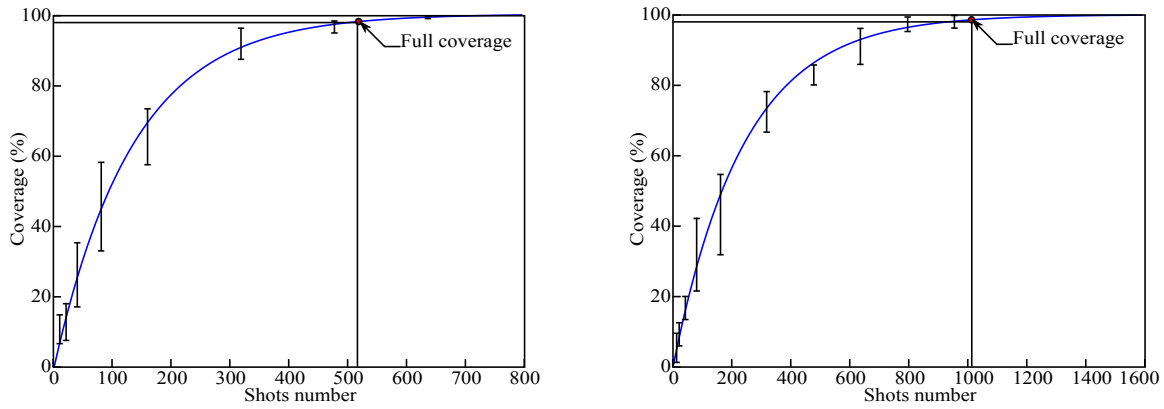

(a) Normal impacts $\theta = 90°$ (b) Oblique impacts $\theta = 45°$

Figure 11: Coverage curves for a thin spring steel plate, corresponding to impingement angles $\theta = 90°$ and $\theta = 45°$ and shot velocity $V = 55$ m/s

In conclusion, the exposure time is taken into account in the numerical model through the corresponding shot number that ensures the same coverage value on the REV peening surface. To be able to compare experimental and numerical results, this paper advises to work with dimensionless parameters. Since N linearly depends on the exposure time T, N/N_f is equivalent to T/T_f, where T_f is the full coverage exposure time.

Figure 12 summarizes the different steps of the proposed methodology to model a real shot peening process.

4. Determination of control curves

This section details the method to obtain the control curves relating the Almen intensity to the shot velocity for a given type of shots and different impingement angles. Determination of these curves is based on the calculation of the residual stress field induced by a number of impacts on an Almen strip. Three types of Almen strips exist: type N for low intensities, type A for intermediate intensities and type C for high intensities [50]. The use of one or other type of Almen strip leads to different control curves. In this work, Almen strip of type A is retained because it is widely used in automotive and aeronautic industries. The associated mechanical properties as well as the Johnson–Cook constants are given in table 1 [22].

Table 1: Mechanical properties and Johnson-Cook constants of SAE 1070 spring steel (taken from [22])

Mechanical properties			Johnson-Cook constants				
Young's modulus E	Poisson's ratio ν	Density ρ	A	B	C	n	m
205 GPa	0.29	7800 Kg/m^3	1408 MPa	600.8 MPa	0.0134	0.234	0

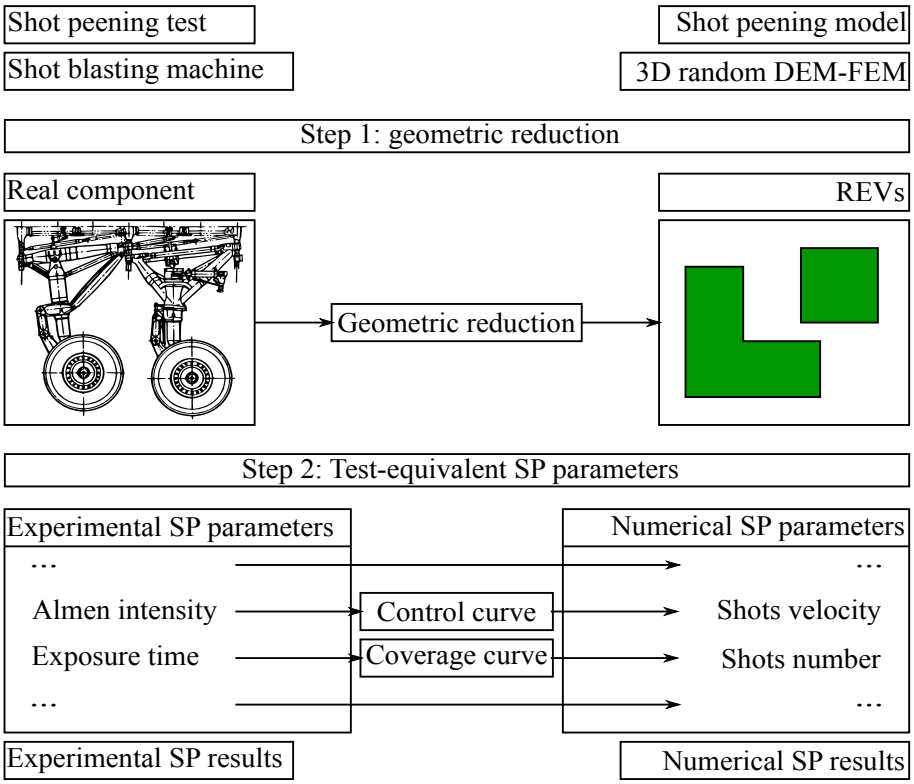

Figure 12: Methodology steps to simulate real shot peening process

Having selected the type of Almen strip, the control curves depend on the type of shots and the impingement angle. In the present paper, steel shots of diameter $D = 0.58\,\text{mm}$ and density $\rho_s = 7800\,\text{Kg/m}^3$, known as $S\,230$, are chosen. This type of shots is widely used to peen Almen strips of type A. It should be recalled that these shots are assumed to be rigid in the present paper. Three impingement angles are also chosen, for which the control curves will be determined: 45° (heavily oblique impacts), 67.5° (intermediate oblique impacts) and 90° (normal impacts). This allows to get an idea of how the control curves evolve according to impingement angle, and then to obtain rapidly approximate curves associated to other intermediate angles.

In summary, three control curves will be obtained in this section, using Almen strips of type A, $S\,230$ shots and three different impingement angles $\theta = \{45°, 67.5°, 90°\}$. To this end, a great number of simulations will be performed. Indeed, for each impingement angle, different values of Almen intensity corresponding to different impact velocities must be determined. Four impact velocities V are used in this paper: 25 mm/s, 35 mm/s, 45 mm/s and 55 mm/s. For each of these velocities, different numbers of shots (dual exposure time parameter) will be used to obtain the corresponding peening arc heights. The numbers of shots N used here are: 10, 20, 40, 80, 160, 320 and 480 shots. Furthermore, since the initial coordinates of the shots are randomly generated, each simulation will be repeated 6 times using different sequences S of shots, to study the random aspects of the peening process. To optimize the computation time, this part is automated using *Python* language. Figure 13 presents the associated algorithm.

4.1. Almen strip modeling

The great number of simulations presented in figure 13 are very time-consuming. The use of entire models of the Almen strip can be crippling, especially very fine mesh must be used to capture the peening-induced residual stresses and to correctly predict the resulting arc heights. To overcome this problem, several techniques have been developed in the literature [14, 22]. Among them, the model proposed by Guagliano [14] is retained in this paper. In this model, the Almen strip is modeled by a small representative elementary volume (REV) having the same thickness of the strip. Then, analytical model is applied to compute the Almen strip arc height from the peening-induced residual stress in this REV. To properly obtain the REV xy-dimensions (peening surface dimensions),

```
For θ in [45, 67.5, 90]
    For V in [25, 35, 45, 55]
        For N in [10, 20, 40, 80, 160, 320, 480]
            For S in [1, 2, 3, 4, 5, 6]
                Call python to generate the random shot sequence
                Call python to modify the Abaqus input file
                Call abaqus server for computation
                Call python for post-processing
```

Figure 13: *Python* algorithm to obtain the control curves

the method proposed in subsection 3.1 will be applied. Although the optimal *xy*-dimensions depend on the shot velocity and impingement angle, for practical purposes, only one REV will be used for all the simulations. The *xy*-dimensions of this REV will be computed based on the two extreme cases: normal impacts with maximal shot velocity and heavily oblique impacts with maximal shot velocity. The largest *xy*-dimensions obtained from these cases will be retained as *xy*-dimensions of the REV peening surface.

For each of the above cases, several sufficiently distant two-shot impacts were performed on a large plate having the same material and thickness as for the considered Almen strip (fig. 14). Starting with adjacent ones, the two shots in these impacts were gradually moved away, to obtain the minimal distance d_{min} from which impacts do not influence each other. Figures 14a and 14b present the associated results of stress regions around impacts. Based on these figures, the minimal distances associated with normal and oblique impacts are respectively $d_{min} = 2\,D$ and $d_{min} = 1.5\,D$, with D being the shot diameter. Therefore, the dimensions of the REV used for all the simulations are: $6\,D \times 6\,D \times h$, with h being the thickness of the modeled Almen strip. Symmetric boundary conditions are applied on the lateral sides, whereas embedding conditions are applied on the bottom surface. Simulations using this REV allow predicting the peening-induced residual stress distributions σ_x^{ind} in this element. For each of these simulations, σ_x^{ind} is averaged over the whole *xy*-plane of the measuring region ($2\,D \times 2\,D \times h$ region at the REV center). The averaged residual stress profile $\hat{\sigma}_x^{ind}$ (which is only function of z) is then assumed to be uniformly distributed over the whole Almen strip, fixed to the Almen block (mounting fixture). However, this is not sufficient to predict the associated Almen intensity (required to obtain the control curves). Indeed, it is not directly possible to predict the residual arc height of the strip by knowing only the residual stresses due to impacts in the fixed strip.

4.2. Arc height calculation

In fact, after release of the rigid constraints due to the support and the bolts, the originally straight Almen strip becomes curved and modifies the residual stress field (fig. 15). This is because the peening-induced residual stresses are not in self-equilibrium, due to boundary conditions, and tend to stretch and bend the strip. To prevent these effects, compressive force F_x and bending moment M_y are applied on the strip by the fixing support to maintain the strip straight. Note that, due to the ratio of length to width of the Almen strip, only longitudinal curvature is considered (transverse curvature effects are neglected here).

Using elasticity theory, F_x and M_y can be expressed as [14]:

$$F_x = \int_S \hat{\sigma}_x^{ind}(z)\, dS \tag{6}$$

$$M_y = \int_S \hat{\sigma}_x^{ind}(z)\, z\, dS \tag{7}$$

where S is the Almen strip section. The removal of the bolts can therefore be simulated by applying on this strip a force and a moment of equal value and opposite sign with respect to F_x and M_y. Accordingly, the residual stress in the released (curved) Almen strip can be expressed using the elasticity theory as [14]:

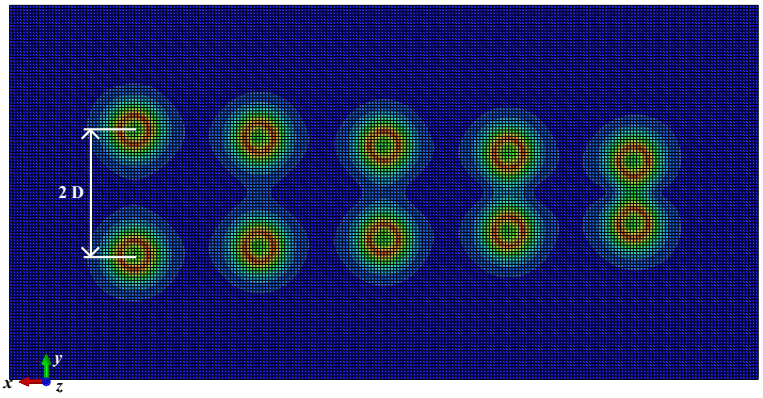

(a) Von Mises residual stress state due to normal impacts $\theta = 90°$

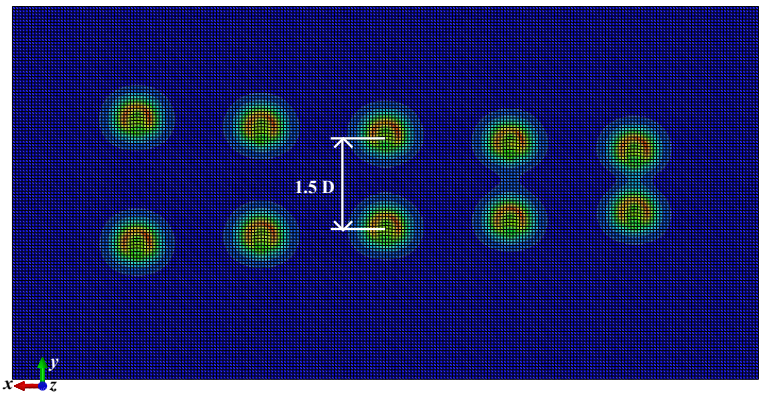

(b) Von Mises residual stress state due to oblique impacts $\theta = 45°$

Figure 14: Determination of the minimal distance between two shots to ensure independence between two impacts

$$\hat{\sigma}_x^{res}(z) = \hat{\sigma}_x^{ind}(z) - \frac{F_x}{S} - \frac{M_y}{I_y} z \tag{8}$$

$I_y = \frac{b h^3}{12}$ is the second moment of inertia with respect to $y-$axis, b and h are respectively the strip dimensions along $y-$axis and $z-$axis. After determining F_x and M_y, it is possible to compute the residual arc height Ah. Based on reference [25], F_x has practically no influence on Ah which can be expressed as:

$$Ah \quad = \quad \frac{M_y}{2\,E\,I_y}\left(\frac{l}{2}\right)^2 \quad = \quad \frac{3\,M_y\,l^2}{2\,E\,b\,h^3} \tag{9}$$

where E is the Almen strip Young's modulus, l is the reference distance for Almen intensity measuring. As specified in the standards [50], the Almen gauge measures the arc height between two specific points of the strip, *i.e.* $l = 31.75\,\text{mm}$ and not the total Almen strip length as used in some papers. The arc height given by (9) is only due to longitudinal curvature, the effect of the transverse curvature is not considered. Figure 16 presents the evolution of arc height versus shot number (dual exposure time parameter), corresponding to $V = 55\,\text{m/s}$ and two different impact angles. As when using exposure time [55], this evolution can be expressed as:

$$Ah\,(N) = \frac{B}{(N+d)^p} - \frac{B}{d^p} \tag{10}$$

where B, d and p are fitting parameters which can be determined using the Least Square (LS) method. Using (10),

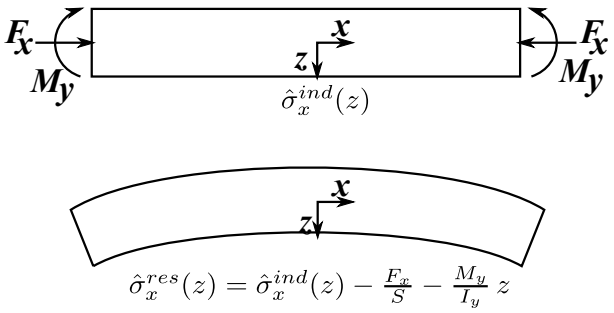

Figure 15: Almen strip deformation after bolts removal

the associated Almen intensity can be determined by solving:

$$Ah\,(2\,N) = 1.1\,Ah\,(N) \tag{11}$$

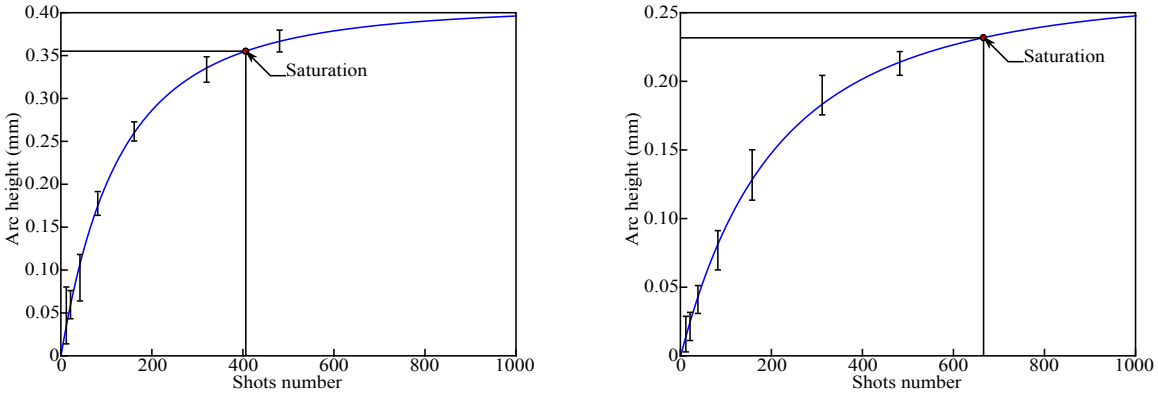

(a) Normal impacts $\theta = 90°$ (b) Oblique impacts $\theta = 45°$

Figure 16: Saturation curves of an Almen strip of type A, corresponding to impingement angles $\theta = 90°$ and $\theta = 45°$, and shot velocity $V = 55\,\mathrm{m/s}$

Applying (11) on the results of the different simulations presented in figure 13, the control curves associated with the S 230 shots and the impingement angles $\theta = \{45°, 67.5°, 90°\}$ can be obtained (fig. 17). These curves will be used to determine the numerical shot velocity that ensures the experimental Almen intensity. A comparison between the numerical and experimental [52, 22] control curves for $\theta = 90°$ is given in figure (fig. 17). These curves are in close agreement for relatively low shot velocities V, however they drift away as V increases. This can be explained by the fact that at high velocities the effects of the shot collisions (ignored in the present model) become significant. The use of the numerically obtained control curves would reduce errors due to such effects. Indeed, they allow to obtain the effective shot velocity that leads to the expected (experimentally measured) Almen intensity which is a key indicator of the effectiveness and repeatability of a given SP process.

5. Validation

In the previous sections, a simplified 3D random DEM-FEM coupling model was developed to simulate the process of shot peening at minimal cost. Using this model, a comprehensive methodology was proposed to correctly predict the residual stresses due to real SP test in the target component. The present section aims to validate these model and methodology. To this end, a shot peening experiment from the literature [57] is reproduced numerically. This experiment consists in peening an aluminum $Al\,7075-T\,73$ disk specimen of diameter 25.4 mm and thickness 9.5 mm with $S\,230$ steel shots during several minutes to ensure 200 % coverage. The corresponding impingement

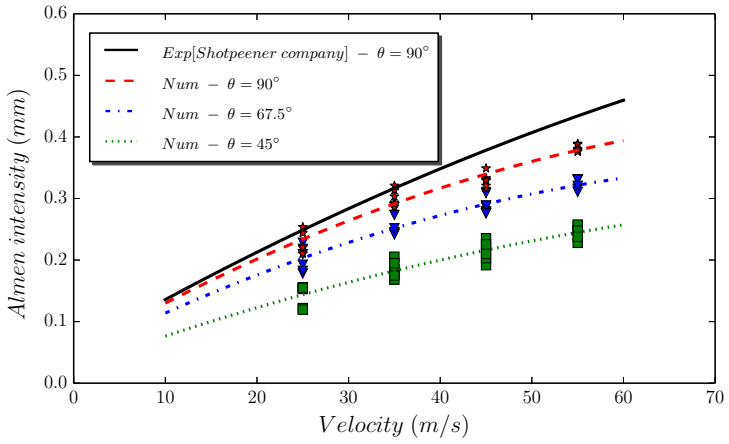

Figure 17: Numerical control curves obtained using S 230 shots and three different impingement angles $\theta = \{45°, 67.5°, 90°\}$; and experimental control curve obtained using S 230 shots and impingement angle $\theta = 90°$ (taken from [52, 22])

angle is $\theta = 65° \pm 5°$ and the Almen intensity is $12\,A$ (*i.e.* 0.3 mm saturation arc height obtained using an Almen strip of type A).

The first step of the proposed methodology consists in determining the representative elementary volumes (REVs) so as to correctly represent the target component. Given the simplicity of the disk specimen, only one REV at the center of this specimen is used. To determine the peening surface dimensions, the method explained in subsection 3.1 is applied. After simulation of several two-shot impacts with different distances between shots, the minimal distance from which impacts do not influence each other is found to be $d_{min} = 1.5$ mm. Therefore, the REV peening surface is chosen as a square of 4.5 mm × 4.5 mm dimensions. Since the considered specimen is relatively thin, the REV thickness is chosen to be the same that the real thickness. Symmetric boundary conditions are applied on the lateral sides, whereas embedding conditions are applied on the bottom surface. This REV is modeled with FEM using the Johnson-Cook model. Table 2 provides the associated mechanical properties as well as the Johnson-Cook constants. After convergence study, the selected REV is discretized such that a fine mesh of 0.025 mm×0.025 mm×0.025 mm dimensions is applied in a small region near to the top surface, whereas gradually coarsened mesh is applied in the rest of the REV domain.

Table 2: Mechanical properties and Johnson-Cook constants of aluminum $Al\,7075 - T\,73$ (taken from [58])

Mechanical properties			Johnson-Cook constants				
Young's modulus E	Poisson's ratio ν	Density ρ	A	B	C	n	m
71 GPa	0.33	2780 Kg/m^3	434 MPa	303.58 MPa	0	0.39	0

Concerning the process parameters, the shot velocity corresponding to $12\,A$ Almen intensity has to be determined firstly. Since the experimental impingement angle is $\theta = 65° \pm 5°$, the control curve associated with $\theta = 67.5°$ (fig. 17) is used to obtain an approximate value of this velocity. Based on this control curve (fig. 17), the shot velocity corresponding to Almen intensity $12\,A$ (0.3 mm) is found to be $V = 47$ m/s. After determining the shot velocity, the number of shots N_c ensuring 200% coverage has to be determined. To this end, a single-shot impact on the selected REV with velocity $V = 47$ m/s and impact angle $\theta = 65°$ is simulated to determine the individual indentation area. Using this area, N_c (corresponding to 200% coverage) can be determined as explained in subsection 3.2.2. Figure 18 shows the coverage evolution as function of shot number. The full coverage shot number N_f is around 725 shots. Therefore, to ensure 200% coverage, $N_c = 2\,N_f$ must be used ($N_c = 1450$ shots). The N_c initial positions of the shots are randomly generated as explained in section 2. To investigate the random effects on the peening induced residual stresses, two different sequences of N_c shots are generated. Using DEM, these shots are modeled by rigid spheres of diameter $D = 0.58$ mm and density $\rho_s = 7800$ Kg/m^3.

After simulations, the peening-induced residual stresses in the specimen REV associated with the two shot

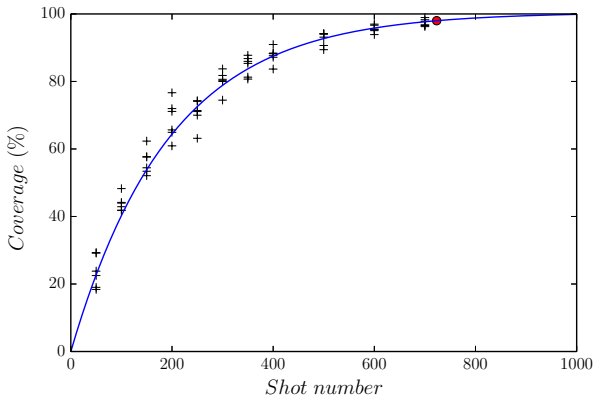

Figure 18: Coverage curve of the selected specimen REV

sequences are given in figure 19. Comparison between these numerical results shows that, when sufficient number N of shots is used, the random effects on the simulation results are insignificant. Therefore, in such a case, there is no need to repeat a given simulation several times to take average results. To draw conclusions on the validity of the proposed numerical model as well as the associated methodology, the obtained numerical results are compared to the experimental ones [57], as illustrated in figure 19. The predicted residual stresses are of the same order of magnitude as those obtained experimentally. A 8% discrepancy is found between the maximal numerical and experimental residual stress. This difference may be due to the simplified constitutive law used to describe the REV mechanical behavior. Indeed, the $Al\,7075 - T\,73$ Johnson-Cook model we could find in the literature [58] includes neither strain rate effects nor thermal effects ($C = 0$ and $m = 0$, table 2). Given the complexity of the shot peening process, such discrepancy could be acceptable. Therefore, it can be concluded that the proposed methodology has enabled to offset the effects of the simplifying assumptions used to develop the DEM-FEM model. By following this methodology, the proposed SP model can be used to simulate a real shot peening process.

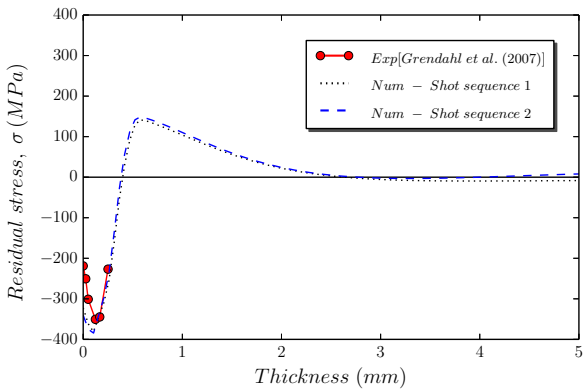

Figure 19: Numerical residual stresses in the specimen REV calculated with two different shots sequences; and the experimental residual stresses obtained by Grendahl *et al.* [57]

6. Conclusion

The present work tried to give a comprehensive methodology to simulate a real shot peening process with minimal computation effort. First, the main classes of the existing numerical models were briefly reviewed and criticized to identify their main advantages. These advantages were then used to developed a new SP numerical model aiming to properly simulate a real shot peening process. A 3D random DEM-FEM coupling model was proposed. The target component is modeled using FEM to correctly model its mechanical response, whereas DEM

is used to model the shots, which are considered as rigid spheres, to avoid unaffordable computation times when using large shot numbers.

After developing the coupling model, a comprehensive methodology adapted to this model was proposed to correctly simulate a real SP process. This methodology consists of two steps. The first step aims to reduce the target component geometry by selecting sufficiently representative elementary volumes of this component. To correctly adjust the REVs dimensions, a numerical method was proposed as an alternative to the conventional approach of convergence study which requires a prior knowledge of the shot number and positions. The second step of the proposed methodology consists in determining the test-equivalent SP parameters to be applied on the selected REVs. Almost all the shot parameters and component parameters are independent of the size of the target component, and are easy to model. However, this is not the case for the process parameters, especially the Almen intensity and the exposure time, which cannot be directly taken into account in the numerical model. Since these two parameters ensure the effectiveness and repeatability of a given SP process, they must be correctly modeled to properly simulate this process. To take into account the Almen intensity in the proposed REV model, this paper proposes to search numerical control curves relating this parameter to shot velocity for given shot type and Almen strip. Even if experimental control curves exist, the use of curves obtained with the proposed numerical model is preferred to reduce errors due to numerical simplifications. Concerning the exposure time, this parameter can be regarded as dual coverage parameter. Therefore, it is sufficient to consider the resulting coverage in the numerical model to take into account this parameter. To this end, a numerical model inspired by the standard experimental method of visual inspection was proposed to determine relationship between coverage and shot number. This relationship can then be used to determine the shot number that ensures the expected coverage (exposure time) on the REV.

To validate the proposed model and the associated methodology, they were applied to simulate a real shot peening experiment from the literature. In order to study the random effects of the shots generation, the SP simulation was repeated two times using different randomly generated shot sequences. The numerical results obtained using these sequences are in very close agreement which proves that for relatively large shot number the random effects are insignificant. Furthermore, these results compare favorably with the experimental ones which proves the validity of the proposed model and methodology to simulate a real shot peening process.

Finally, the proposed methodology, which can be easily extended to other numerical models taking into account more SP mechanisms, presents a major step towards quantitative simulation of industrial shot peening experiments at affordable costs.

Acknowledgements

This work was financially supported by *Héroux-Devtek Inc.* and the *Natural Sciences and Engineering Research Council of Canada (NSERC)*. The authors would like to thank Arnaud Divialle, R&T Team Lead, for helpful comments on the manuscript.

References

[1] K. Kloos, E. Macherauch, Development of Mechanical Surface Strengthening Processes from the Beginning until Today, in: 3rd International Conference on Shot Peening, Garmisch-Partenkirchen, Germany , 1987, pp. 3–27.

[2] G. Farrahi, J. Lebrun, D. Couratin, Effect of Shot Peening on Residual Stress and Fatigue Life of Spring Steel , Fatigue & Fracture of Engineering Materials & Structures 18 (2) (1995) 211–220.

[3] M. Guagliano, S. Bagheri, I. F. Parienete, R. Ghelichi, Effects of severe air blast shot peening on microstructure and residual stress state of Al alloys , Key Engineering Materials 417-418 (2010) 393–396.

[4] I. Pariente, M. Guagliano, About the role of residual stresses and surface work hardening on fatigue ΔKth of a nitrided and shot peened low-alloy steel, Surface and Coatings Technology 202 (2008) 3072–3080.

[5] S. Kyriacou, Shot Peening Mechanics, A Theoretical Study, in: Proceedings of the 6th International Conference, IOM Communications, Oxford, 1996, pp. 505–516.

[6] A. Niku-Lari, Shot Peening, in: 1st International Conference on Shot Peening, Paris, France, 1981, pp. 1–21.

[7] H. Lieurade, A. Bignonnet, Fundamental aspects of the effect of shot peening on the fatigue strength of metallic parts and structures, in: 3rd International Conference on Shot Peening, Garmisch-Partenkirchen, Germany , 1987, pp. 343–360.

[8] H. Wohlfahrt, Shot Peening and Residual Stresses, in: E. Kula, V. Weiss (Eds.), Residual Stress and Stress Relaxation, Vol. 28 of Sagamore Army Materials Research Conference Proceedings, Springer US, 1982, pp. 71–92.

[9] G. Maeder, L. Castex, J. Barralis, Précontraintes et traitements superficiels, Techniques de l'ingénieur [M1180].

[10] M. Kobayashia, T. Matsuia, Y. Murakamib, Mechanism of creation of compressive residual stress by shot peening, International Journal of Fatigue 20 (5) (1998) 351–357.

[11] B. Bhuvaraghana, M. Sivakumar, O. Prakash, Overview of the effects of shot peening on plastic strain, work hardening and residual stresses, in: W. Oster (Ed.), Computational materials, Nava science, 2009.

[12] S. Al-Hassani, Mechanical aspects of residual stress development in shot peening, in: 1st International Conference on Shot Peening, Paris, France, 1981.

[13] S. T. S. Al-Hassani, An Engineering Approach To Shot Peening Mechanics, in: 2nd International Conference on Shot Peening, Chicago, USA, 1984, pp. 275–282.

[14] M. Guagliano, Relating Almen intensity to residual stresses induced by shot peening: a numerical approach, Journal of Materials Processing Technology 110 (2001) 277–286.

[15] H. Guechichi, Prévision des contraintes résiduelles dues au grenaillage de précontrainte, Ph.D. thesis, École Nationale Supérieure des Arts et Métiers (1986).

[16] S. P. Timoshenko, J. N. Goodier, Theory of elasticity.

[17] M. T. Khabou, L. Castex, G. Inglebert, Effect of Material Behaviour Law on the Theoretical Shot Peening Results, European Journal of Mechanics A/Solids 9 (6) (1990) 537–549.

[18] R. Fathallah, G. Inglebert, L. Castex, Prediction of plastic deformation and residual stresses induced in metallic parts by shot peening, Journal of Materials Science & Technology 14 (1998) 631–639.

[19] K. J. Li, M. Yao, D. Wang, R. Z. Wang, Effect of ion beam bombardment on the carbide in M2 steel modified by ion-beam-assisted deposition , Materials science and engineering A 147 (1) (1991) 77–80.

[20] S. Shen, Z. D. Han, C. A. Herrera, S. N. Atluri, Final Report-U.S., Department of Transportation: Federal Aviation Administration, FAA Report No. DOT/FAA/AR-03/76.

[21] H. Miao, S. Larosea, C. Perrona, M. Lévesque, An analytical approach to relate shot peening parameters to Almen intensity, Surface and Coatings Technology 205 (7) (2010) 2055–2066.

[22] B. Bhuvaraghana, S. Srinivasanb, B. Maffeo, Numerical simulation of Almen strip response due to random impacts with strain-rate effects, International Journal of Mechanical Sciences 53 (6) (2011) 417–424.

[23] T. Honga, J. Ooia, B. Shawb, A numerical study of the residual stress pattern from single shot impacting on a metallic component, Advances in Engineering Software 39 (2008) 743–756.

[24] T. Honga, J. Ooia, B. Shawb, A numerical simulation to relate the shot peening parameters to the induced residual stresses, Engineering Failure Analysis 15 (2008) 1097–1110.

[25] H. Miao, S. Larose, C. Perron, M. Lévesque, On the potential applications of 3D random finite element model for simulation of shot peening, Advances in Engineering Software (2009) 1023–1038.

[26] K. Han, D. Peric, D. Owen, J. Yu., A combined finite/discrete element simulation of shot peening processes - Part II: 3D interaction laws, Engineering Computations 17 (23) (2000) 680–702.

[27] K. Murugaratnam, S. Utili, N. Petrinic, A combined DEM-FEM numerical method for shot peening parameter optimization, Advances in Engineering Software 79 (2015) 13–26.

[28] S. Meguid, G. Shagal, J. Stranart, 3D FE analysis of peening of strain-rate sensitive materials using multiple impingement model, International Journal of Impact Engineering 27 (2002) 119–134.

[29] M. Jebahi, F. Dau, J. L. Charles, I. Iordanoff, Multiscale Modeling of Complex Dynamic Problems: An Overview and Recent Developments, Archives of Computational Methods in Engineering (2014) 1–38.

[30] M. Jebahi, D. André, I. Terreros, I. Iordanoff, Discrete Element Method to Model 3D Continuous Materials, Wiley, 2015.

[31] O. C. Zienkiewicz, R. L. Taylor, The Finite Element Method for Solid and Structural Mechanics, Elsevier, 2005.

[32] P. S. Follansbee, G. B. Sinclair, Quasi-static normal indentation of an elasto-plastic half-space by a rigid sphere - I: Analysis, International Journal of Solids and Structures 20 (1) (1984) 81–91.

[33] G. B. Sinclair, P. S. Follansbee, K. L. Johnson, Quasi-static normal indentation of an elasto-plastic half-space by a rigid sphere - II: Results, International Journal of Solids and Structures 21 (8) (1985) 865–888.

[34] E. R. Kral, K. Komvopoulos, D. B. Bogy, Elastic-Plastic Finite Element Analysis of Repeated Indentation of a Half-Space by a Rigid Sphere, Journal of Applied Mechanics 60 (4) (1993) 829–841.

[35] E. Rouhaud, D. Deslaef, Rigid-Plastic Finite Element Simulation of Peening Process with Plastically Deforming Shot, Materials science forum 404 (2002) 153–158.

[36] H. L. Zion, W. S. Johnson, Parametric Two-Dimensional Finite Element Investigation: Shot Peening of High-Strength Steel , Journal of The American Institute of Aeronautics and Astronautics 44 (9) (2006) 1973–1982.

[37] A. Gariépy, S. Larose, C. Perron, M. Lévesque, Shot peening and peen forming finite element modelling - Towards a quantitative method, International Journal of Solids and Structures 48 (2011) 2859–2877.

[38] T. Kim, J. H. Lee, H. Lee, S. K. Cheong, An area-average approach to peening residual stress under multi-impacts using a three-dimensional symmetry-cell finite element model with plastic shots, Materials & Design 31 (1) (2010) 50–59.

[39] G. Majzoobi, R. Azizi, A. Alavi Nia, A three-dimensional simulation of shot peening process using multiple shot impacts, Journal of Materials Processing Technology 164-165 (2005) 1226–1234.

[40] R. Evans, Shot peening process: modelling, verification, and optimisation, Materials Science and Technology 18 (8) (2002) 831–839.

[41] M. S. ElTobgy, M. A. Elbestawi, Three-dimensional elastoplastic finite element model for residual stresses in the shot peening process, Proceedings of the Institution of Mechanical Engineers - Part B: Journal of Engineering Manufacture 218 (11) (2004) 1471–1481.

[42] E. Rouhaud, A. Ouakka, C. Ould, M. François, J. L. Chaboche, Un modèle éléments finis pour le grenaillage, les effets d'écrouissage cinématique, 17ème Congrès Français de Mécanique. Troyes, France.

[43] H. Y. Miao, S. Larose, C. Perron, M. Lévesque, Numerical simulation of the stress peen forming process and experimental validation, Advances in Engineering Software 42 (11) (2011) 963–975.

[44] S. M. H. Gangaraj, M. Guagliano, G. H. Farrahi, An approach to relate shot peening finite element simulation to the actual coverage, Surface and Coatings Technology 243 (2014) 39–45.

[45] B. Bhuvaraghan, S. Srinivasan, B. Maffeo, R. McCLain, Y. Potdar, O. Prakash, Shot peening simulation using discrete and finite element methods, Advances in Engineering Software 41 (12) (2010) 1266–1276.

[46] S. Meguid, G. Shagal, J. Stranart, J. Daly, Three dimensional dynamique Finite element analysis of shot peening induced residual stresses, Finite Elements in Analysis and Design 31 (3) (1999) 179–191.

[47] Abaqus Analysis User's Manual, Abaqus 6.13, Dassault Systemes.

[48] J. Almen, P. Black, Residual Stresses and Fatigue in Metals, McGraw-Hill, 1963.

[49] SAE Standard J443 - Procedures for using standard shot peening test strip.

[50] SAE Standard J442 - Test strip, holder, and gage for shot peening.

[51] SAE Standard AMS 2430 - Shot peening, Automatic.

[52] Shotpeener company, Shot size and speed to achieve Almen intensity, http://www.shotpeener.com/learning/ref.php.

[53] H. Y. Miao, D. Demers, S. Larose, C. Perron, M. Lévesque, Experimental study of shot peening and stress peen forming, Journal of Materials Processing Technology 210 (2010) 2089–2102.

[54] SAE Standard J2277 - Shot Peening Coverage, Developed by Surface Enhancement Committee.

[55] S. Karuppanan, J. Romero, E. de los Rios, C. Rodopoulos, A. Levers, A Theoretical and Experimental Investigation into the Development of Coverage in Shot Peening, in: Proceedings of the 8th International Conference on shot peening, 2002, pp. 101–107.

[56] D. Kirk, M. Abyaneh, Theoretical Basis of Shot Peening Coverage Control, in: Proceeding of second International Conference on Shotpenning, Chicago, 1993, pp. 183–190.

[57] S. Grendahl, D. Snoha, B. Hardisky, Shot-Peening Sensitivity of Aerospace Materials, Tech. rep., Army Research Laboratory, Aberdeen Proving Ground, MD 21005-5069 (2007).

[58] Y. Yang, D. H. Li, H. G. Zheng, X. M. Li, J. F., Self-organization behaviors of shear bands in 7075 T73 and annealed aluminum alloy, Materials Science and Engineering A 527 (1-2) (2009) 344–354.